PERGAMON

Computers & Fluids 32 (2003) 47–57

computers & fluids

www.elsevier.com/locate/compfluid

A 3D mathematical model for the prediction of mucilage dynamics

Alessandra Jannelli [a], Riccardo Fazio [a,*], Davide Ambrosi [b]

[a] *Dipartimento di Matematica, Università di Messina, Salita Sperone 31, I-98166 Messina, Italy*
[b] *Dipartimento di Matematica, Politecnico di Torino, Corso Duca degli Abruzzi 24, 10129 Torino, Italy*

Accepted 26 June 2001

Abstract

We illustrate a three-dimensional mathematical model for the prediction of biological processes that typically occur in a sea region with minor water exchange. The model accounts for particle transport due to water motion, turbulent diffusion and reaction processes and we use a fractional-step approach for discretizing the related different terms.

Keywords: 3D ecological model; Advection diffusion reaction equations; Splitting numerical method; Mucilage dynamics

1. Introduction

In the last years mathematical modeling and numerical simulation of reacting species in a fluid became a theme of increasing environmental interest. Intensive efforts spent in predicting the evolution of the mucilage in the Adriatic sea, notably for the events that lead to highest concentrations [8], constitute a good example of this increased interest.

A simple but reasonable mathematical model for the prediction of biological processes that occur in the Adriatic sea, is the following:

* Corresponding author. Fax: +39-090-393502.
E-mail address: rfazio@dipmat.unime.it (R. Fazio).

0045-7930/03/$ - see front matter
PII: S0045-7930(01)00100-1

$$\begin{aligned}
&\frac{\partial}{\partial t}(\rho c_1) + \nabla\cdot(\rho c_1 \mathbf{v}) - \nabla\cdot(\mu_1 \nabla c_1) = \alpha \frac{c_1 c_2^2}{1+\beta c_2^2} - \gamma c_1^2,\\
&\frac{\partial}{\partial t}(\rho c_2) + \nabla\cdot(\rho c_2 \mathbf{v}) - \nabla\cdot(\mu_2 \nabla c_2) = -\delta \frac{c_1 c_2^2}{1+c_2^2},\\
&\frac{\partial}{\partial t}(\rho c_3) + \nabla\cdot(\rho c_3 \mathbf{v}) - \nabla\cdot(\mu_3 \nabla c_3) = \varphi \frac{c_1^2}{1+\psi c_1^2},
\end{aligned} \tag{1}$$

endowed by suitable initial and boundary conditions. Here $c_1(\mathbf{x},t)$, $c_2(\mathbf{x},t)$ and $c_3(\mathbf{x},t)$ represent the grass–weed population, their nutrients and mucilage concentrations, respectively. In general the water density ρ depends on the temperature and salinity, but this variation has a minor effect on the problem at hand. Thus, for the sake of simplicity, in the following we assume a constant value of ρ and take it equal to one. The right-hand side terms are $\alpha c_1 c_2^2/(1+\beta c_2^2)$, grass–weed logistic growth; $-\gamma c_1^2$, natural death for the grass–weed; $-\delta c_1 c_2^2/(1+c_2^2)$, loss of c_2 for the consumption due to c_1; $\varphi c_1^2/(1+\psi c_1^2)$, mucilage growth due to the grass–weed production [9]. The constants α, β, γ, δ, φ and ψ should be determined according to experimental results.

The velocity field $\mathbf{v}(\mathbf{x},t) = (u,v,w)^{\mathrm{T}}$ is to be supplied in order to solve Eq. (1) and could be possibly evaluated by a mathematical model that accounts for the hydrodynamics [1]. As the mucilage is not uniformly distributed along the vertical, a hydrodynamic model giving the three-dimensional (3D) flow field must be preferred and, in this respect, the depth-integrated mathematical models (shallow water models) should be discarded.

The diffusion coefficients μ_1, μ_2 and μ_3 account for turbulent diffusion, which are typically much more relevant than the molecular ones for the problems under interest. A rigorous evaluation of these coefficients is a very intricate matter, we just refer to [6] for a survey of the literature on this issue.

The model (1) is a time-dependent system of partial differential equations in three spatial dimensions. It takes into account physical and biological processes modeled by three distinct terms:

1. the interaction of the species essentially described by reaction terms (e.g., growth of species, consumption of nutrients, etc.),
2. the motion of each component due to the turbulent nature of the flow field, modeled by the (turbulent) diffusion terms,
3. the transport of each component due to the motion of the water, described by the advection terms.

2. Numerical methods

In the present paper we consider a fractional step approach to solve numerically the system of Eq. (1). Such a method consists in decoupling, in the discretized equations, the steps corresponding to the advection, diffusion and reaction processes. This splitting is possible when a loose coupling exists between these phenomena so that to each of them is associated with a different characteristic time. In our case such kind of assumption holds and the use of a fractional step seems to be promising, as it allows for adopting the optimal numerical approach to each term of the equations.

We rewrite (1) in the vectorial form $\mathbf{c}_t = A(\mathbf{c}) + D(\mathbf{c}) + R(\mathbf{c})$, where we denote by $A(\mathbf{c})$, $D(\mathbf{c})$ and $R(\mathbf{c})$ the advection, diffusion and reaction terms, respectively. To apply a fractional step method several possibilities are available. For instance, it is possible to use the following Strang splitting [7]:

1. starting with a reference solution $\mathbf{c}^n$ at time t^n, solve $\mathbf{c}_t = A(\mathbf{c})$ over $\Delta t/2$,
2. use the obtained approximate solution and solve $\mathbf{c}_t = D(\mathbf{c})$ over $\Delta t/2$,
3. use the obtained approximate solution and solve $\mathbf{c}_t = R(\mathbf{c})$ over Δt,
4. use the obtained approximate solution and solve $\mathbf{c}_t = D(\mathbf{c})$ over $\Delta t/2$,
5. use the obtained approximate solution and solve $\mathbf{c}_t = A(\mathbf{c})$ over $\Delta t/2$ to get the approximate solution $\mathbf{c}^{n+1}$ at time t^{n+1}.

As far as the accuracy question is concerned, by using the Strang splitting technique we obtain second order accuracy in time provided that each sub-problem is solved by a second order accurate method [7]. Because of the nonlinearity of the problem, the stability conditions may vary as the solution evolves. Given a Δt^n, each of the five steps of the above splitting procedure must be stable for Δt^n, otherwise it is necessary to go back to reduce the current time step.

2.1. Advection term: $\mathbf{c}_t = A(\mathbf{c})$

In this section we consider a proper discretization of the advection term

$$\begin{aligned} &\frac{\partial c_1}{\partial t} + \nabla \cdot (c_1 \mathbf{v}) = 0, \\ &\frac{\partial c_2}{\partial t} + \nabla \cdot (c_2 \mathbf{v}) = 0, \\ &\frac{\partial c_3}{\partial t} + \nabla \cdot (c_3 \mathbf{v}) = 0. \end{aligned} \tag{2}$$

Eq. (2) are three uncoupled convection equations for the three species. A huge body of literature exists about accurate numerical solutions of these equations so that it is convenient to state first the aspects that characterize the problem at hand. In our opinion, two mandatory requirements arise: the discretization of (2) must be conservative and monotone. As the hydrodynamical terms are responsible for variation in space and time of the species field, although they do affect their total quantity, *conservation* means that the amount of each species in the computational domain must be preserved by the numerical scheme. *Monotonicity* means that no numerical instabilities should affect the results, yielding spurious oscillations and eventually to negative (meaningless) concentrations.

In order to satisfy all the requirements mentioned above we consider a second order finite volume method given within the CLAWPACK software, a set of Fortran routines, available on Internet [4], for solving systems of conservation laws. The method is based on solving one-dimensional (1D) Riemann problems at cell edges while applying flux-limiter function to suppress oscillations. Multi-dimensional transport is modeled using wave-propagation approach in which the flux at each cell interface is built up on the basis of information on the propagation in the direction of the interface from neighboring cells.

The method can be written in the form

$$\mathbf{c}_{i,j,k}^{n+1} = \mathbf{c}_{i,j,k}^{n} + \Delta_{i,j,k}^{\mathrm{up}} - \frac{\Delta t}{\Delta x}\left(\widetilde{\mathbf{F}}_{i+\frac{1}{2},j,k}^{n} - \widetilde{\mathbf{F}}_{i-\frac{1}{2},j,k}^{n}\right) - \frac{\Delta t}{\Delta y}\left(\widetilde{\mathbf{G}}_{i,j+\frac{1}{2},k}^{n} - \widetilde{\mathbf{G}}_{i,j-\frac{1}{2},k}^{n}\right) - \frac{\Delta t}{\Delta z}\left(\widetilde{\mathbf{H}}_{i,j,k+\frac{1}{2}}^{n} - \widetilde{\mathbf{H}}_{i,j,k-\frac{1}{2}}^{n}\right),$$

where the first order upwind correction is defined by

$$\Delta_{i,j,k}^{\mathrm{up}} = -\frac{\Delta t}{\Delta x}\left(u^{-}\,\Delta\mathbf{c}_{i+1,j,k} + u^{+}\,\Delta\mathbf{c}_{i,j,k}\right) - \frac{\Delta t}{\Delta y}\left(v^{-}\,\Delta\mathbf{c}_{i,j+1,k} + v^{+}\,\Delta\mathbf{c}_{i,j,k}\right) - \frac{\Delta t}{\Delta z}\left(w^{-}\,\Delta\mathbf{c}_{i,j,k+1} + w^{+}\,\Delta\mathbf{c}_{i,j,k}\right).$$

The numerical fluxes $u^{\pm}\,\Delta\mathbf{c}$, $v^{\pm}\,\Delta\mathbf{c}$ and $w^{\pm}\,\Delta\mathbf{c}$ result from solving the 1D Riemann problem along normal direction to each cell interface in the x-direction, y-direction and z-direction.

On the other hand, the numerical fluxes $\widetilde{\mathbf{F}}$, $\widetilde{\mathbf{G}}$ and $\widetilde{\mathbf{H}}$ are used to perform second order correction terms, transverse propagations and the corner transports as showed by LeVeque [5]. For simplicity, only contributions to fluxes coming from solution of the Riemann problem in the x-direction will be discussed in detail. The contributions from the other two sets of Riemann problems are obtained in a similar manner with a change of the roles of fluxes.

The second order update is written as a correction to the flux, as in standard flux-limiter methods

$$\widetilde{\mathbf{F}}_{i+\frac{1}{2},j,k} = \frac{1}{2}\left|u_{i+\frac{1}{2},j,k}\right|\left(1 - \frac{\Delta t}{\Delta x}\left|u_{i+\frac{1}{2},j,k}\right|\right)\Delta\mathbf{c}_{i,j,k}\,\Phi_{i,j,k}, \tag{3}$$

where $\Phi_{i,j,k}$ is the limiter that depends on the nature of the solution locally.

The multi-dimensional transport is characterized by splitting each flux differences $u^{\pm}\,\Delta\mathbf{c}_{i,j,k}$, determined by solving the Riemann problem in x-direction, into two transverse flux differences $v^{+}u^{\pm}\,\Delta\mathbf{c}_{i,j,k}$ and $v^{-}u^{\pm}\,\Delta\mathbf{c}_{i,j,k}$. These are used to modify the nearby $\widetilde{\mathbf{G}}$ fluxes,

$$\begin{aligned}
\widetilde{\mathbf{G}}_{i-\frac{1}{2},j+\frac{1}{2},k} &:= \widetilde{\mathbf{G}}_{i-\frac{1}{2},j+\frac{1}{2},k} - \frac{1}{2}\frac{\Delta t}{\Delta x}v^{+}u^{+}\,\Delta\mathbf{c}_{i,j,k},\\
\widetilde{\mathbf{G}}_{i-\frac{1}{2},j-\frac{1}{2},k} &:= \widetilde{\mathbf{G}}_{i-\frac{1}{2},j-\frac{1}{2},k} - \frac{1}{2}\frac{\Delta t}{\Delta x}v^{-}u^{+}\,\Delta\mathbf{c}_{i,j,k},\\
\widetilde{\mathbf{G}}_{i-\frac{3}{2},j+\frac{1}{2},k} &:= \widetilde{\mathbf{G}}_{i-\frac{3}{2},j+\frac{1}{2},k} - \frac{1}{2}\frac{\Delta t}{\Delta x}v^{+}u^{-}\,\Delta\mathbf{c}_{i,j,k},\\
\widetilde{\mathbf{G}}_{i-\frac{3}{2},j+\frac{1}{2},k} &:= \widetilde{\mathbf{G}}_{i-\frac{3}{2},j-\frac{1}{2},k} - \frac{1}{2}\frac{\Delta t}{\Delta x}v^{-}u^{-}\,\Delta\mathbf{c}_{i,j,k}.
\end{aligned} \tag{4}$$

In the same manner, the flux differences $u^{\pm}\,\Delta\mathbf{c}_{i,j,k}$ are split into transverse flux differences in the z-direction in order to obtain $w^{\pm}u^{\pm}\,\Delta\mathbf{c}_{i,j,k}$. These are used to modify the nearby $\widetilde{\mathbf{H}}$ fluxes. Once the transverse corrections have been implemented, we proceed propagating also the second order corrections in the transverse direction. Then, also these corrections are splitting, in the y-direction, into up-going and down-going portions in exactly the same manner as $u^{\pm}\,\Delta\mathbf{c}_{i,j,k}$ are split into $v^{+}u^{\pm}\,\Delta\mathbf{c}_{i,j,k}$ and $v^{-}u^{\pm}\,\Delta\mathbf{c}_{i,j,k}$. The same is done in the z-direction.

In 3D algorithm additional transverse terms are included into corner cells. These terms, called "corner transport" ones, are implemented by splitting each of the four terms $v^{\pm}u^{\pm}\,\Delta\mathbf{c}_{i,j,k}$ in the z-direction, yielding $w^{+}v^{\pm}u^{\pm}\,\Delta\mathbf{c}_{i,j,k}$ and $w^{-}v^{\pm}u^{\pm}\,\Delta\mathbf{c}_{i,j,k}$, which requires solving four more Riemann problems. These term are used to update fluxes according to

$$
\begin{aligned}
\widetilde{\mathbf{H}}_{i-\frac{1}{2},j-\frac{1}{2},k+\frac{1}{2}} &:= \widetilde{\mathbf{H}}_{i-\frac{1}{2},j-\frac{1}{2},k+\frac{1}{2}} + \frac{1}{6}\frac{\Delta t}{\Delta x}\frac{\Delta t}{\Delta y} w^{+}v^{+}u^{+}\,\Delta\mathbf{c}_{i,j,k} - \frac{1}{6}\frac{\Delta t}{\Delta x}\frac{\Delta t}{\Delta y} w^{+}v^{-}u^{+}\,\Delta\mathbf{c}_{i,j,k},\\
\widetilde{\mathbf{H}}_{i-\frac{1}{2},j-\frac{1}{2},k-\frac{1}{2}} &:= \widetilde{\mathbf{H}}_{i-\frac{1}{2},j-\frac{1}{2},k-\frac{1}{2}} + \frac{1}{6}\frac{\Delta t}{\Delta x}\frac{\Delta t}{\Delta y} w^{-}v^{+}u^{+}\,\Delta\mathbf{c}_{i,j,k} - \frac{1}{6}\frac{\Delta t}{\Delta x}\frac{\Delta t}{\Delta y} w^{-}v^{-}u^{+}\,\Delta\mathbf{c}_{i,j,k},\\
\widetilde{\mathbf{H}}_{i-\frac{1}{2},j+\frac{1}{2},k+\frac{1}{2}} &:= \widetilde{\mathbf{H}}_{i-\frac{1}{2},j+\frac{1}{2},k+\frac{1}{2}} - \frac{1}{6}\frac{\Delta t}{\Delta x}\frac{\Delta t}{\Delta y} w^{+}v^{+}u^{+}\,\Delta\mathbf{c}_{i,j,k},\\
\widetilde{\mathbf{H}}_{i-\frac{1}{2},j+\frac{1}{2},k-\frac{1}{2}} &:= \widetilde{\mathbf{H}}_{i-\frac{1}{2},j+\frac{1}{2},k-\frac{1}{2}} - \frac{1}{6}\frac{\Delta t}{\Delta x}\frac{\Delta t}{\Delta y} w^{-}v^{+}u^{+}\,\Delta\mathbf{c}_{i,j,k},\\
\widetilde{\mathbf{H}}_{i-\frac{1}{2},j-\frac{3}{2},k+\frac{1}{2}} &:= \widetilde{\mathbf{H}}_{i-\frac{1}{2},j-\frac{3}{2},k+\frac{1}{2}} + \frac{1}{6}\frac{\Delta t}{\Delta x}\frac{\Delta t}{\Delta y} w^{+}v^{-}u^{+}\,\Delta\mathbf{c}_{i,j,k},\\
\widetilde{\mathbf{H}}_{i-\frac{1}{2},j-\frac{3}{2},k-\frac{1}{2}} &:= \widetilde{\mathbf{H}}_{i-\frac{1}{2},j-\frac{3}{2},k-\frac{1}{2}} + \frac{1}{6}\frac{\Delta t}{\Delta x}\frac{\Delta t}{\Delta y} w^{-}v^{-}u^{+}\,\Delta\mathbf{c}_{i,j,k}.
\end{aligned}
\tag{5}
$$

Six similar updates are made to the cells to the left of the interface by replacing $\left(i-\frac{1}{2}\right)$ with $\left(i-\frac{3}{2}\right)$ and replacing $u^{+}\,\Delta\mathbf{c}_{i,j,k}$ by $u^{-}\,\Delta\mathbf{c}_{i,j,k}$ in the above expression. In addition, the four terms $w^{\pm}u^{\pm}\,\Delta\mathbf{c}_{i,j,k}$, used in the updates of the nearby $\widetilde{\mathbf{H}}$ fluxes, must be split in y-direction, yielding $v^{-}w^{\pm}u^{\pm}\,\Delta\mathbf{c}_{i,j,k}$ and $v^{+}w^{\pm}u^{\pm}\,\Delta\mathbf{c}_{i,j,k}$. These are then used to update neighboring $\widetilde{\mathbf{G}}$ fluxes in a manner analogous to (5).

The above discretization automatically satisfies the conservation requirement. This can be seen summing up all the $\mathbf{c}^{n}_{i,j,k}$ (for fixed n). The monotonicity depends on the discretization adopted for the flux.

As Fig. 1 shows, the x-component of velocity $u_{i+\frac{1}{2},j,k}$, the y-component of velocity $v_{i,j+\frac{1}{2},k}$, and the z-component of velocity $w_{i,j,k+\frac{1}{2}}$ are centered at the right, back and top face of the cell, respectively, whereas the concentrations $\mathbf{c}_{i,j,k}$ are located at the center. This is the so-called marker-and-cell (MAC) method [3].

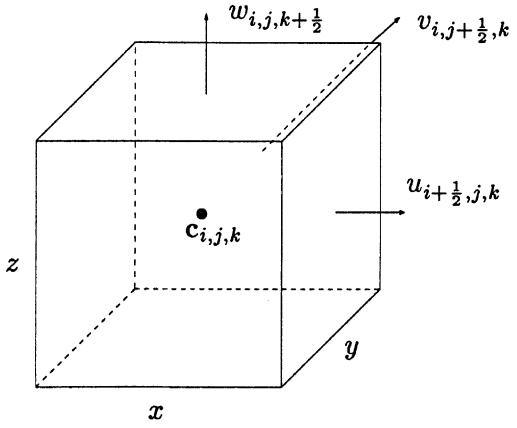

Fig. 1. Location of velocity and concentration information in a MAC mesh cell.

2.2. Diffusion term: $\boldsymbol{c}_t = D(\boldsymbol{c})$

In this section we consider a proper discretization of the diffusion term

$$\begin{aligned}
&\frac{\partial c_1}{\partial t} - \nabla \cdot (\mu_1 \nabla c_1) = 0,\\
&\frac{\partial c_2}{\partial t} - \nabla \cdot (\mu_2 \nabla c_2) = 0,\\
&\frac{\partial c_3}{\partial t} - \nabla \cdot (\mu_3 \nabla c_3) = 0.
\end{aligned} \tag{6}$$

Eq. (6) represents three uncoupled diffusion equations for the three species. The diffusion term is discretized implicitly to avoid using small time steps when this is not dictated by considerations of accuracy in detecting the correct dynamics of the population. As for the stability, the following Crank–Nicolson scheme

$$\mathbf{c}^{n+1}_{i,j,k} - \frac{\Delta t}{2\,\Delta x\,\Delta y\,\Delta z}\mathbf{w}^{n+1}_{i,j,k} = \mathbf{c}^{n}_{i,j,k} + \frac{\Delta t}{2\,\Delta x\,\Delta y\,\Delta z}\mathbf{w}^{n}_{i,j,k}, \tag{7}$$

where

$$\mathbf{w}^{n}_{i,j,k} = -\left\{ \Delta y\,\Delta z\left(\widehat{\mathbf{F}}^{n}_{i+\frac{1}{2},j,k} - \widehat{\mathbf{F}}^{n}_{i-\frac{1}{2},j,k}\right) + \Delta x\,\Delta z\left(\widehat{\mathbf{G}}^{n}_{i,j+\frac{1}{2},k} - \widehat{\mathbf{G}}^{n}_{i,j-\frac{1}{2},k}\right) + \Delta x\,\Delta y\left(\widehat{\mathbf{H}}^{n}_{i,j,k+\frac{1}{2}} - \widehat{\mathbf{H}}^{n}_{i,j,k-\frac{1}{2}}\right)\right\} \tag{8}$$

with

$$\begin{aligned}
\widehat{\mathbf{F}}_{i+\frac{1}{2},j,k} &= -\mu_{i+\frac{1}{2},j,k}\frac{\mathbf{c}_{i+1,j,k} - \mathbf{c}_{i,j,k}}{\Delta x},\\
\widehat{\mathbf{G}}_{i,j+\frac{1}{2},k} &= -\mu_{i,j+\frac{1}{2},k}\frac{\mathbf{c}_{i,j+1,k} - \mathbf{c}_{i,j,k}}{\Delta y},\\
\widehat{\mathbf{H}}_{i,j,k+\frac{1}{2}} &= -\mu_{i,j,k+\frac{1}{2}}\frac{\mathbf{c}_{i,j,k+1} - \mathbf{c}_{i,j,k}}{\Delta z},
\end{aligned} \tag{9}$$

is unconditionally stable. This method is second order accurate in space and in time. The linear system obtained is solved by the bi-conjugate gradient method [2, pp. 362–379]. Fig. 2 shows the matrix of coefficients on a sample domain of $3 \times 4 \times 5$ mesh points.

2.3. Reaction term: $\boldsymbol{c}_t = R(\boldsymbol{c})$

The evolution in time of the species due to the reaction term is governed by

$$\frac{\mathrm{d}\mathbf{c}}{\mathrm{d}t} = \mathbf{r}, \tag{10}$$

where, $\mathbf{r}^{\mathrm{T}} = \left(\alpha c_1 c_2^2/(1+\beta c_2^2) - \gamma c_1^2, -\delta c_1 c_2^2/(1+c_2^2), \varphi c_1^2/(1+\psi c_1^2)\right)$. Here, we consider the simple explicit second order Taylor method

$$\mathbf{c}^{n+1} = \mathbf{c}^{n} + \Delta t\,\mathbf{r}(\mathbf{c}^{n}) + \frac{1}{2}\Delta t^2\left[\frac{\partial \mathbf{r}}{\partial \mathbf{c}}\mathbf{r}\right](\mathbf{c}^{n}). \tag{11}$$

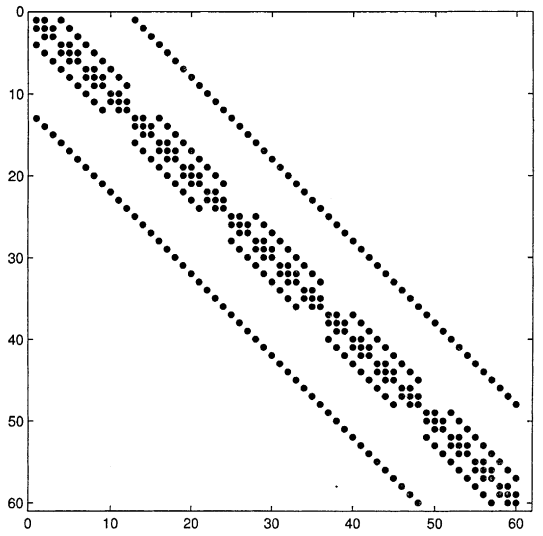

Fig. 2. Example of matrix of coefficients for the Crank–Nicolson method.

3. Sample numerical results

In this section we set $\mu_1 = 0.1$, $\mu_2 = 1$, $\mu_3 = 0.1$, $\alpha = 6.6$, $\beta = 1$, $\gamma = 10$, $\delta = 0.5$, $\varphi = 10$ and $\psi = 1$. The results presented are determined on a computational domain $L_x \times L_y \times L_z$ with $\Delta x = \Delta y = \Delta z = 1$, and a variable time step Δt^n chosen to ensure a Courant number of about 0.9. We always apply the Van Leer flux-limiter function for each wave.

In order to mimic the 3D circulation of a basin in a simple problem, we consider the following velocity field:

$$\begin{aligned} u &= \omega_1 x(x - L_x)\left(y - \frac{L_y}{2}\right) + \omega_2 x(x - L_x)\left(z - \frac{L_z}{2}\right), \\ v &= -\omega_1 y(y - L_y)\left(x - \frac{L_x}{2}\right), \\ w &= -\omega_2 z(z - L_z)\left(x - \frac{L_x}{2}\right), \end{aligned} \tag{12}$$

with $\omega_1 = 0.01$, $\omega_2 = 0.001$ and $L_x = 100$, $L_y = 40$, $L_z = 5$. This velocity field satisfies the divergence-free condition: $u_x + v_y + w_z = 0$ and provides a periodic circulation. The values of ω_1 and ω_2 are chosen in order to have approximately an unitary period.

Fig. 3 shows the velocity field within the plane $z = 5$ and resembles qualitatively the real circulation within the northern Adriatic sea (see Fig. 1 in [8]). Note that at the upper surface of the water the velocity field has zero z-component.

As a test case, we assume as initial conditions that there are no mucilage (c_3) within the domain, a uniform distribution of nutrient (c_2) and a concentration of grass–weed (c_1) localized only within a part of the domain:

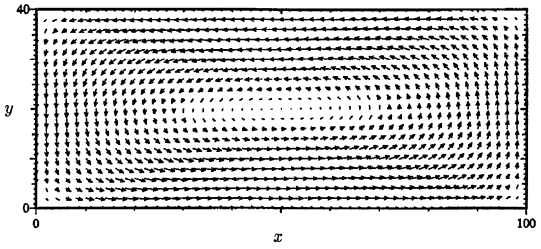

Fig. 3. Velocity field within the plane $z = 5$.

$$\begin{aligned} c_1(x,y,z,0) &= \begin{cases} 1 & \text{for } 28 \leqslant x \leqslant 32 \quad 16 \leqslant y \leqslant 20 \quad 3 \leqslant z \leqslant 5, \\ 0 & \text{elsewhere,} \end{cases} \\ c_2(x,y,z,0) &= 1 \quad \text{everywhere,} \\ c_3(x,y,z,0) &= 0 \quad \text{everywhere.} \end{aligned} \tag{13}$$

Moreover, we apply Neumann boundary conditions corresponding to no diffusive flux; the convective one vanishes too because the velocity component normal to the boundary is null. The Figs. 4–7 display the evolution of the concentrations at the upper surface of the sea. The numerical results show that the mucilage field c_3 is different from zero only in that part of the domain

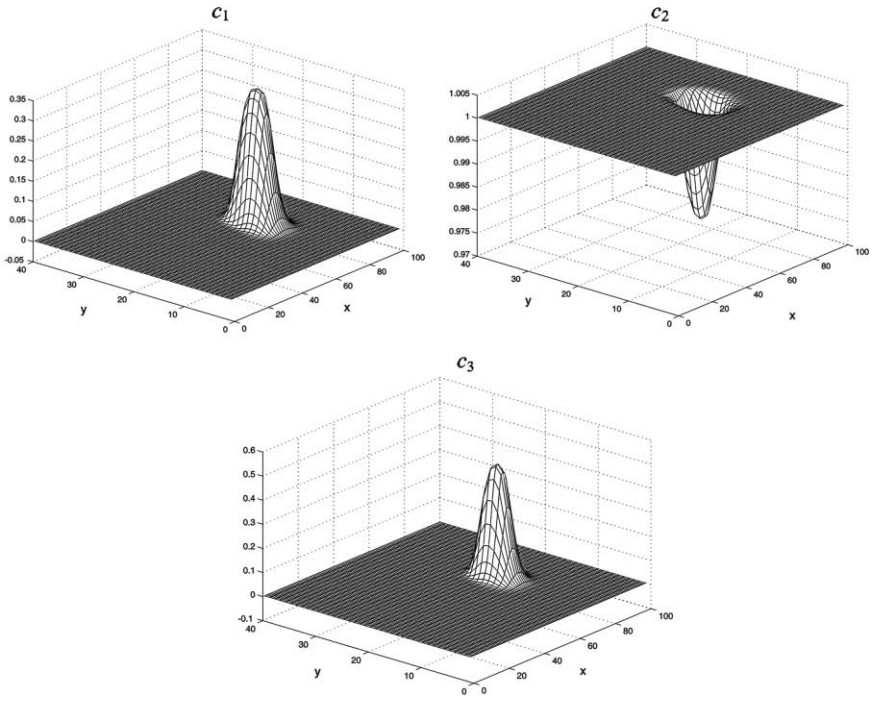

Fig. 4. Concentrations at $t = 0.3$.

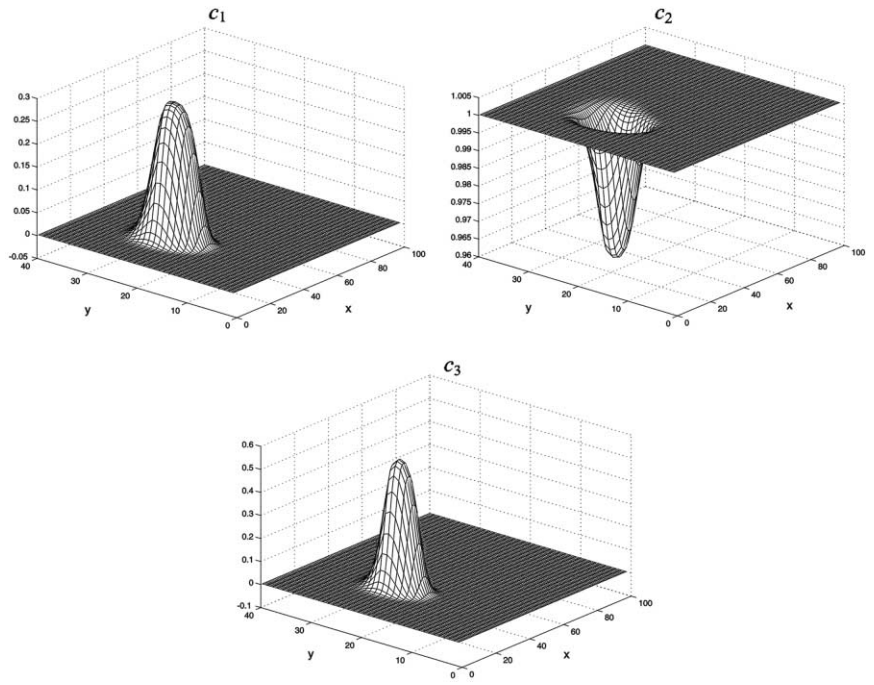

Fig. 5. Concentrations at $t = 0.6$.

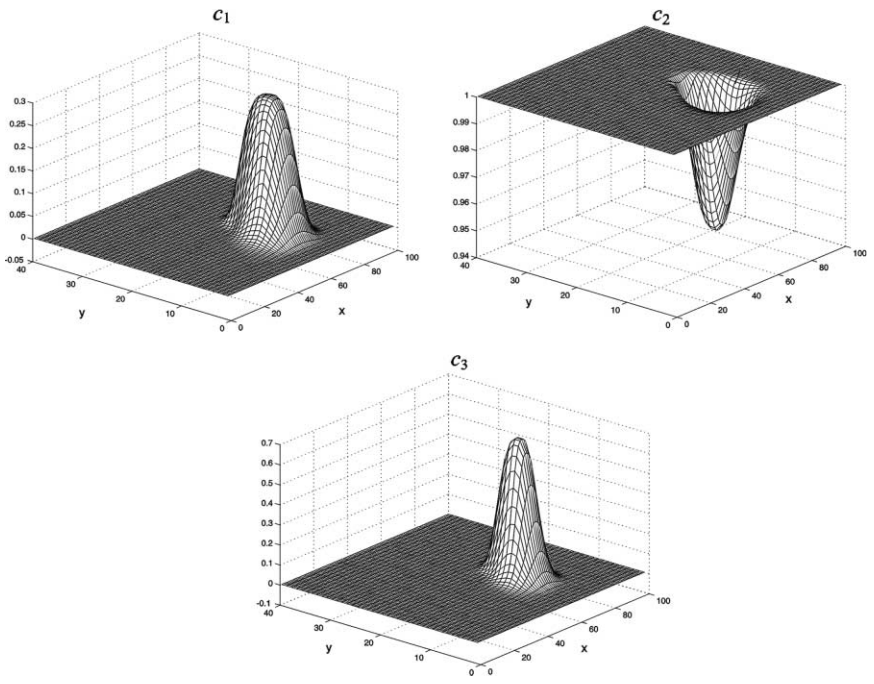

Fig. 6. Concentrations at $t = 0.9$.

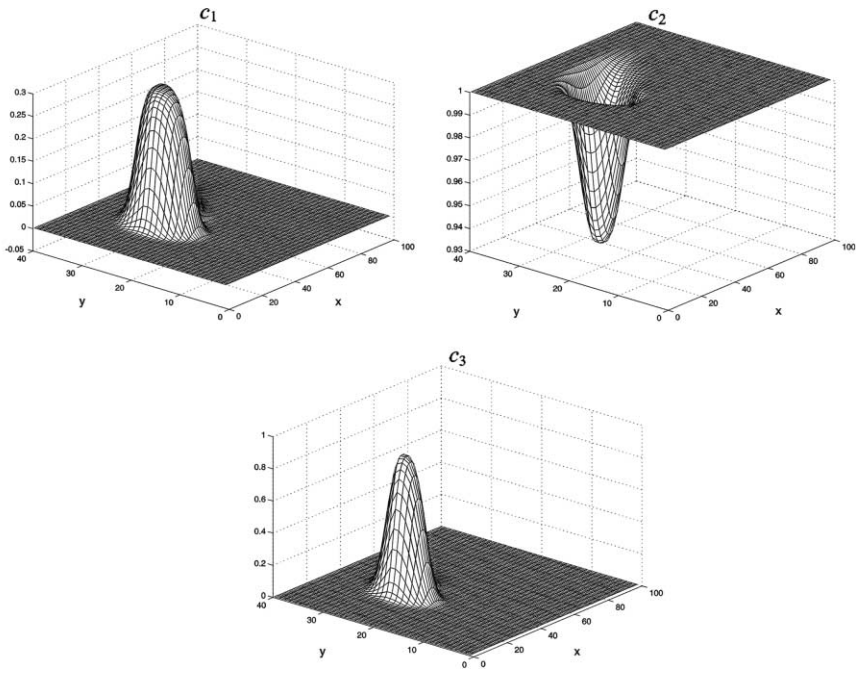

Fig. 7. Concentrations at $t = 1.2$.

where c_1 and c_2 coexist. Its localization changes as c_1 moves according to the circulation of the assigned velocity field.

On biological ground, because of the consumption of nutrients due to c_1, we would expect that, fixed a point in the path of c_1, the concentration c_2 will be a decreasing function of time, during the interaction between c_1 and c_2. No source term for c_2 is considered in this test case. As a consequence, in a long time period, we should observe a deformation of the bell shapes of the concentrations. Actually, this is confirmed by the numerical results (contrast Fig. 4 with Fig. 7).

4. Conclusions

In recent years, the Adriatic sea has occasionally suffered high mucilage concentration, causing relevant economic and ecological damages. In this paper, is proposed a first possible model linking biology and hydrodynamic to predict this phenomenon.

Combining physical and biological processes, into the same mathematical model, we obtain a time-dependent system of partial differential equations in three spatial dimensions. In order to solve this model numerically, we use a fractional step approach where the solution procedure is split up into distinct steps solved independently by the most suitable methods. The numerical results confirm the qualitatively expected behavior.

Several items remain to be developed. First of all, the crude hydrodynamical description of this paper should be substituted by a 3D calculation of the flow field. Secondly, the mucilage is to grow abruptly in the Adriatic sea when the circulation is very small. A most interesting issue

would then be to investigate if this kind of mathematical model is able to reproduce, at least qualitatively, the influence of the hydrodynamical aspects that is observed in the abrupt growth of the mucilage.

Acknowledgement

Work supported by CNR through the project PRISMA2.

References

[1] Ambrosi D. Mathematical models for free-surface enviromental flow. Technical report, CRS4, 1994.
[2] Golub GH, van Loan CF. Matrix computations. 2nd ed. London: Hopkins University Press; 1989.
[3] Harlow FH, Welsh JE. Numerical calculation of time-dependent viscous incompressible flow with free surface. Phys Fluids 1965;8:2182–9.
[4] LeVeque RJ. CLAWPACK software. Available form: netlib.att.com in netlib/pdes/claw.
[5] LeVeque RJ. Wave propagation algorithms for multi-dimensional hyperbolic systems. J Comput Phys 1995;1:1–81.
[6] Rodi F. Turbulence models and their applications in hydraulics: a state of art review. In: IAHR Monographs. Amsterdam: Balkema; 1984.
[7] Strang G. On the construction and comparison of difference schemes. SIAM J Num Anal 1968;5:506–17.
[8] Thornton DCO, Santillo D, Thake B. Prediction of sporadic mucilaginous algal blooms in the northern Adriatic sea. Mar Pollut Bull 1999;38:891–8.
[9] Tyson R, Stern LG, LeVeque RJ. Fractional step methods applied to a chemotaxis model. J Math Biol 2000;5: 455–75.